Listeria monocytogenes **encodes a functional ESX-1 secretion system whose expression is detrimental to *in vivo* infection**

Jorge Pinheiro[1,2,3]*, Olga Reis[1,2,3]*, Ana Vieira[1,2]*, Ines M. Moura[1,2]*, Luisa Zanolli Moreno[1,2,4], Filipe Carvalho[1,2,3], M. Graciela Pucciarelli[5,6], Francisco García-del Portillo[5], Sandra Sousa[1,2] and Didier Cabanes[1,2,#]

[1] Instituto de Investigação e Inovação em Saúde – i3S, Universidade do Porto, Porto, Portugal
[2] Group of Molecular Microbiology, Instituto de Biologia Molecular e Celular - IBMC, Porto, Portugal
[3] Instituto de Ciências Biomédicas Abel Salazar, Universidade do Porto, Porto, Portugal
[4]Laboratório de Saúde Pública, Faculdade de Saúde Pública, Universidade de São Paulo, São Paulo, Brazil.
[5]Centro Nacional de Biotecnología-CSIC (CNB-CSIC), Madrid, Spain.
[6]Departamento de Biología Molecular, Universidad Autónoma de Madrid. Centro de Biología Molecular 'Severo Ochoa' (CBMSO-CSIC). Madrid, Spain.
* Equally contributed to the work
[#] Corresponding author

Corresponding author:

Didier Cabanes
i3S - Instituto de Investigação e Inovação em Saúde , Universidade do Porto
IBMC - Institute for Molecular and Cell Biology
GM2 - Group of Molecular Microbiology
Rua Alfredo Allen, 208
4200-135 Porto, Portugal

Telf: +351 220 408 800 Ext. 6099
e-mail: didier@ibmc.up.pt

Running Title: *Listeria* ESX-1 is detrimental to infection

Keywords: ESX-1 secretion system, *Listeria monocytogenes*, EsxA, ESAT-6, Type VII secretion system

Abstract

Bacterial pathogenicity deeply depends on the ability to secrete virulence factors that bind specific targets on host cells and manipulate host responses. The Gram-positive bacterium *Listeria monocytogenes* is a human foodborne pathogen that remains a serious public health concern. To transport proteins across its cell envelope, this facultative intracellular pathogen engages a set of specialized secretion systems. Here we show that *L. monocytogenes* EGDe uses a specialized secretion system, named ESX-1, to secrete EsxA, a homologue of the virulence determinants ESAT-6 and EsxA of *Mycobacterium tuberculosis* and *Staphylococcus aureus*, respectively. Our data show that the *L. monocytogenes* ESX-1 secretion system and its substrates are dispensable for bacterial invasion and intracellular multiplication in eukaryotic cell lines. Surprisingly, we found that the EssC-dependent secretion of EsxA has a detrimental effect on *L. monocytogenes in vivo* infection.

Introduction

The capacity to secrete proteins is crucial for the pathogenesis of many bacteria. In Gram-positive bacteria, proteins are delivered by highly specialized secretion systems across cell envelope to reach specific targets [1]. A portion of these proteins, including virulence factors, are often secreted by Sec-independent systems. ESX-1, also called WXG100, is a Sec-independent secretion system first described in *Mycobacterium tuberculosis* [2-4]. This system allows the secretion of ≈100 amino-acid-long proteins that lack the classical signal peptide but contain a Trp-X-Gly motif (WXG100 proteins). *M. tuberculosis* ESAT-6 and CFP-10 are prototypes of WXG100 proteins, both encoded by the region of difference 1 (RD1), involved in virulence and described as highly immunogenic proteins [5]. Deletion of the *esx-1* locus abrogates ESX-1-dependent secretion and strongly attenuates the virulence of *M. tuberculosis* [6]. Apart from

mycobacterial species, ESX-1 systems are also found in Firmicutes, among which the *S. aureus* ESX-1 is one of the best-characterized [7, 8]. It comprises genes encoding the canonical ESX-1 substrates (EsxA, EsxB), a membrane-anchored FtsK/SpoIIIE-like ATPase (EssC) essential for the secretion machinery, genes coding for membrane-embedded proteins (EssA, EssB, EssD) required for secretion of ESX-1 substrates, as well as staphylococci-specific ESX-1 substrates (EsxC, EsxD), and modulators of ESX-1 activity (EsaA, EsaB) [7-10]. *S. aureus* EsxA and EsxB share features with the *M. tuberculosis* ESAT-6 and CFP-10, including the presence of a WXG motif and the co-dependent secretion. However, unlike ESAT-6 and CFP-10, EsxA and EsxB do not interact. EsxA dimerizes with itself or associates with EsxC, while EsxB interacts with EsxD [8]. Disruption of key components of the *S. aureus* ESX-1 secretion machinery (EssC) or deletion of *esxA* and *esxB* causes a significant reduction in the ability of *S. aureus* to establish kidney or liver abscesses [7, 9, 11]. Moreover, the *S. aureus* ESX-1 secretion system is required for nasal colonization and virulence in a murine lung pneumonia model [12]. EsxA was also shown to interfere with host cell apoptotic pathways, affecting bacterial survival and mediating *S. aureus* release from host cells [13]. Other ESX-1 substrates, such as EsaC, although dispensable for the establishment of acute infections, are required for the formation of persistent infection [11]. Functional ESX-1 secretion systems were also characterized in *Bacillus anthracis, Bacillus subtilis*, *Actinobacterium* and *Streptomyces coelicolor* [14-17].

Listeria monocytogenes (*Lm*) is a ubiquitous Gram-positive bacterium responsible for listeriosis, a severe opportunistic foodborne disease occurring mainly in immunocompromised individuals, newborn, elderly and pregnant women. Listeriosis is the most frequent cause of hospitalization and death due to the consumption of contaminated food in Europe, and involves high illness costs and quality life losses [18]. Clinical features of listeriosis includes septicemia, meningitis, meningoencephalitis and abortions. This facultative intracellular pathogen has evolved multiple strategies to survive inside phagocytic cells, invade non-phagocytic cells and

spread from cell to cell [19]. Each step of its cell infection cycle depends on specific virulence determinants that play specific roles, most of them being surface or secreted proteins [20, 21]. Genes encoding a potential ESX-1 secretion system were identified in *Lm* [22] and the *Lm* EsxA homologue was previously shown dispensable for *Lm* mouse infection [23]. However, although ESX-1 was postulated to represent a broad Gram-positive secretion system [1], the functionality of this apparatus and its role in infection were never previously investigated in *Listeria*.

Results

Lm encodes a putative ESX-1 secretion system.

In agreement with the model proposed for the ESX-1 secretory apparatus [1, 22] and following bioinformatic analyses (BLAST, TopPred2, ProDom) we determined that the *Lm* ESX-1 locus contains genes coding for: the two canonical WXG100 substrate paralogs EsxA (Lmo0056) and EsxB (Lmo0063), the integral membrane FtsK/SpoIIIE-type ATPase EssC (Lmo0061); EsaA (Lmo0057), a polytopic membrane protein with five predicted transmembrane helices; EssA (Lmo0058) and EssB (Lmo0060), two predicted membrane proteins with respectively one and two transmembrane domains; and EsaB (Lmo0059) and Lmo0062, two putative cytoplasmic proteins (Fig. 1A). Membrane topology or soluble character of proteins encoded by the *Lm* ESX-1 locus was predicted and compared to *M. tuberculosis* and *S. aureus* ESX-1 secretion systems (Fig. 1B). This revealed large similarities with the *S. aureus* ESX-1 systems. However, the two ESX-1 substrates (EsxC and EsxD) and the EssD transmembrane protein described in *S. aureus* are absent in *Lm*. Analysis of complete genome sequences available for different *Listeria* species revealed the high level of conservation of the ESX-1 locus within the *Listeria* genus (Fig. 1A). Of note, *esxB* and *lmo0062* are absent from three non-pathogenic species (*L. welshimeri*, *L. seeligeri* and *L. grayi*).

_Lm_ ESX-1 secretion system is functional although weakly expressed.

To evaluate the expression of the *Lm esx-1* locus, we analyzed by RT-PCR the transcription of genes encoding the two major ESX-1 effectors (*esxA* and *esxB*), and two integral membrane proteins essential for the secretion machinery (*essB* and *essC*) [7-10]. RNAs extracted from bacteria in exponential growth phase in BHI at 37ºC were processed for analysis and results showed that all the genes selected are transcribed in these conditions (Fig. 2A). However, *esxB, essC* and *essB* appeared to be weakly expressed as compared to *esxA* and control genes (*inlA, actA, iap*) encoding known *Lm* virulence factors. We also observed that the expression of *esxA* appeared to decrease upon entry into stationary growth phase, which was confirmed by qRT-PCR (Fig. 2B). We also attempted to assess by qRT-PCR the expression of *esxB* and *essC* during growth in exponential or stationary phases. However, transcript levels appeared insufficient to obtain quantifiable amplification, in particular during the stationary growth phase, thus underlining the weak level of expression of these genes. *esxA* was previously shown to be negatively regulated by SigB in *S. au*reus [24]. SigB being the major regulator of the stationary growth phase, we assessed if the decreased expression of *esxA* upon entry into this phase would be due to SigB regulation. We analyzed by qRT-PCR the expression of *esxA* in a *sigB* deletion mutant as compared to the WT strain during growth in exponential and stationary phases, and showed that in both growth phases *esxA* expression appeared independent of the presence of *sigB* (Fig. 2C). *bsh,* which encodes a bile salt hydrolase, was used as a SigB-dependent control gene [25].

To analyse whether the putative *Lm* ESX-1 system was functional, we constructed a deletion mutant strain for *essC* (Δ*essC*), which encodes a structural protein essential for *S. aureus* ESX-1 functionality [7], as well as the corresponding complemented strain (Δ*essC*+*essC*). Both strains were confirmed by PCR and sequencing, and their growth rate in BHI at 37ºC was comparable to that of the WT (Fig. S1A-B). To test the functionality of the ESX-1 secretion system in *Lm*,

we expressed a myc-tagged EsxA protein (EsxA-myc) in WT bacteria and analyzed its secretion during bacterial growth. Western blot of bacterial culture supernatants showed a band of 11 kDa, the expected size for EsxA-myc, with a higher intensity in the exponential growth phase (Fig. 2D left panel). These results indicate that *Lm* EsxA was secreted in these conditions. We then expressed EsxA-myc in the Δ*essC* and Δ*essC*+*essC* strains and performed the same western blot analysis on proteins from the WT, WT+*esxA-myc*, Δ*essC*, Δ*essC*+*esxA-myc* and Δ*essC*+*essC*+*esxA-myc* total bacterial lysates and culture supernatants in exponential growth phase. In the WT+*esxA-myc* strain, EsxA-myc was detected both in the total lysates and culture supernatants, indicating that the protein is produced and secreted (Fig. 2D right panel). In the Δ*essC*+*esxA-myc* strain, EsxA-myc was absent from the supernatant and retained in total lysates, demonstrating that EsxA is secreted in an EssC-dependent manner. This was confirmed by the complementation of the Δ*essC*+*esxA-myc* mutant that restored the secretion of EsxA-myc (Δ*essC*+*essC*+*esxA-myc* line). Altogether, these results show that *Lm* expresses a functional ESX-1 secretion system, albeit at low levels, and that EsxA secretion requires the putative membrane ATPase EssC.

_Lm_ ESX-1 is dispensable for host cell invasion and intracellular multiplication.

To investigate the role of the ESX-1 system in *Lm* cell invasion and intracellular multiplication, we constructed deletion mutants for *esxA*, that we showed to encode a substrate of *Lm* ESX-1, and *esxB* that encodes another putative ESX-1 substrate [7]. Mutants were confirmed by PCR and sequencing, and their growth rates observed in BHI at 37ºC were comparable to that of the WT (Fig. S1A-B).

The WT, Δ*esxA,* Δ*esxB* and Δ*essC* strains were tested for their capacity to invade epithelial cell lines in which *Lm* entry is mainly mediated by internalin A (InlA) (Caco-2) or InlB (Vero). No significant difference in invasion was observed between mutant and WT bacteria in both cell

lines (Fig. 3A), suggesting that the ESX-1 system is not required for *Lm* invasion of epithelial cells.

To analyse the role of ESX-1 in *Lm* intracellular multiplication, the behaviour of the WT, Δ*esxA,* Δ*esxB* and Δ*essC* strains was studied after internalization in J774 murine macrophage-like cells. All strains grew with similar multiplication rates after uptake (Fig. 3B), indicating that none of these genes is required for *Lm* intracellular replication in macrophage-like cells. Altogether these results indicate that the ESX-1 secretion system is dispensable for *Lm* cell invasion and intracellular multiplication.

ESX-1 activity impairs *Lm* infection.

To analyse the involvement of the ESX-1 system in *Lm* infection *in vivo*, we monitored the number of bacteria in the liver and spleen of mice infected intravenously with Δ*esxA,* Δ*esxB*, Δ*essC* or WT bacteria. Unexpectedly, 72h post-infection, all the mutant strains showed a slight increase in bacterial counts in both organs as compared to WT, which was statistically significant for Δ*esxB* (Fig. 4A), implying that ESX-1 activity might have a negative impact on *Lm* infection.

To investigate the potential role of ESX-1 in the gastrointestinal phase of the infectious process, we performed oral inoculation of mice with the WT, Δ*esxA,* Δ*esxB* and Δ*essC* strains. Three days post-inoculation, mutant strains appeared again to be slightly more virulent than the WT. This increased infection was statistically significant for Δ*esxA* in mouse livers (Fig. 4B).

These data indicate that neither the ESX-1 apparatus nor its substrates are crucial for *Lm* infection in the mouse model. Conversely, they suggest that the expression/function of this secretion system causes an adverse effect in *Lm* pathogenicity.

Overexpression of *esxA* in the context of a functional ESX-1 system is detrimental to *Lm* infection.

To further investigate if the ESX-1 function could have a negative effect on *Lm* infection, we performed intravenous infection of mice with *Lm* overexpressing *esxA* (+*esxA*), together with the WT and Δ*esxA* strains. The *esxA* overexpression in the +*esxA* strain was first confirmed by qRT-PCR (Fig. S2A). Growth rate of the +*esxA* strain in BHI or minimal medium at 37ºC, as well as its cell adhesion and infection capacity were comparable to that of the WT strain (Fig. S2B-C), indicating that *esxA* overexpression has no significant impact on *Lm* growth and cellular infectious properties. Three days post infection the Δ*esxA* mutant appeared slightly more virulent as compared to the WT, as already observed (Fig. 4A), whereas +*esxA* bacteria showed a significant number decrease in both mouse organs (Fig. 5A). Inversely, *esxA* overexpression had no effect on the phenotype of a Δ*essC* mutant that, similarly to the Δ*esxA* mutant, also appeared to colonize more efficiently mouse organs than the WT strain (Fig. 5B). These results demonstrate that the detrimental effect of ESX-1 on *Lm* pathogenicity is due to EsxA secretion and depends on a functional ESX-1 machinery.

The production of IFN-γ and TNF-α by immune cells promotes bacterial clearance and is critical in controlling primary *L. monocytogenes* infections [26]. To investigate if the adverse effect of *esxA* overexpression on *Lm* infection is related with higher levels of host IFN-γ and/or TNF-α, we analysed by qRT-PCR levels of IFN-γ and TNF-α transcripts in the liver of WT or +*esxA*-infected mice. No significant difference was observed regarding expression levels of IFN-γ and TNF-α (Fig. 5C). In addition, to discard any role of IFN-γ in the increased resistance of mice to *esxA* overexpressing *Lm*, WT and IFN-γ knock-out mice (IFN-$\gamma^{-/-}$) were intravenously infected with WT or +*esxA* bacteria. Three days post-infection, bacterial loads were overall higher in the organs of IFN-$\gamma^{-/-}$ than in WT mice (Fig. 5D). These data indicated that IFN-γ deficient mice are more susceptible to *Lm* infection and confirmed the role of IFN-γ

211 in the immune response against *Lm* [27]. In line with data observed in BALB/c mice (Fig. 5A),
212 the +*esxA* strain showed significant infection attenuation in both organs of WT mice as
213 compared to *Lm* WT bacteria (Fig. 5D). However, this infection defect was similar in IFN-γ
214 deficient animals, suggesting that IFN-γ is not involved in the increased resistance of mice to
215 *Lm* overexpressing *esxA*.
216

217 **Discussion**

218 The analysis of the bacterial ability to secrete proteins to or beyond their surface is crucial in
219 the understanding of bacterial pathogenesis. In *M. tuberculosis* and *S. aureus,* ESX-1 and its
220 substrates were shown to play an important role in virulence [5, 7]. ESX-1 appears to be very
221 conserved in *Listeria*, in particular among pathogenic species, and only partially present in the
222 majority of non-pathogenic *Listeria* species.
223 We showed that the ESX-1 locus of *L. monocytogenes* EGDe is expressed in standard growth
224 conditions, with *esxA* appearing more expressed than *esxB*, *essB* and *essC*. These results are in
225 agreement with previous transcriptional analyses [28] and are consistent with the presence of a
226 transcription terminator between *esxA* and *esaA*. This could suggest a different transcriptional
227 regulation between *esxA* and the other ESX-1 genes. Regarding the expression of ESX-1 genes
228 in different conditions, no change were observed when bacteria were grown at 37ºC, 25ºC or
229 7ºC [29, 30], nor in presence of 6% NaCl [29], nor when grown at pH5 [31], nor when grown in culture
230 media supplemented with glucose, cellobiose or glycerol [32, 33]. In addition, as compared to
231 bacteria grown in BHI at 37ºC, the expression of the ESX-1 locus appears also unchanged in
232 *Listeria* recovered from infected murine macrophages [34, 35], or from mouse intestinal lumen [36]
233 and spleens [37]. Interestingly, the entire ESX-1 locus was shown as up-regulated after
234 incubation of *Lm* in human blood [36], and *essC* and *esxC* were also shown as up-regulated

during cell infection [34]. Altogether, these results indicate that the ESX-1 locus of *L. monocytogenes* EGDe is poorly or not expressed in most of the conditions, with some genes of the locus expressed in few conditions that could suggest a role of the ESX-1 apparatus in these specific environments.

Using a deletion mutant and complemented strain for *essC*, we demonstrated that ESX-1 is functional in *Lm*, at least for the secretion of EsxA. Even if EssC was shown to be an essential ESX-1 element also for the secretion of EsxB in *M. tuberculosis* and *S. aureus* [5, 7], the EssC-dependent secretion of EsxB remains to be confirmed in *Lm*. EsxA and EsxB are the only WXG100 proteins predicted to be encoded by the *Lm* genome. In addition to EsxA and EsxB, the EsxC protein is also a substrate for ESX-1 in *S. aureus* and confers pathogenic function to this bacterium [11]. However, an *esxC* ortholog is absent from *Lm*. Instead, an unrelated gene of unknown function (*lmo0062*) occupies the *esxC* position in the *Lm* genome (Fig. 1). Interestingly, Lmo0062 was recently predicted to be secreted [38], therefore investigating its capacity to be secreted in an ESX-1-dependent manner could widen the spectrum of ESX-1 substrates to proteins that do not belong to the WXG100 family.

All the above observations induced a strong presumption for the involvement of ESX-1 in *Lm* pathogenicity. However, we demonstrated that this secretion system and its substrates are not required for *Lm* cell invasion, intracellular multiplication and *in vivo* infection. In agreement with our results, EsxA was also previously shown dispensable for *Lm* mouse infection [23]. Unexpectedly, we observed a slight increase in the infection level of mutants for ESX-1 components as compared to WT bacteria. This was also previously observed for a Δ*esxA* mutant [23], suggesting a damaging role for ESX-1 in *Listeria* infectious capacity. In agreement with this hypothesis, overexpression of *esxA* resulted in a decrease infection of *Lm* in the mouse model, confirming the adverse effect of a functional ESX-1 secretion system. Despite our attempts to elucidate the reasons of this detrimental role, we failed to find differences

regarding host immune responses upon infection by WT or *esxA* overexpressing *Lm*. ESAT-6 (the mycobacterial EsxA homolog) was shown to play a pro-apoptotic role in *M. tuberculosis* [39]. A comparable role of *Lm* EsxA could result in increased bacterial recognition and clearance by the host immune system that would explain the phenotype of *esxA* overexpressing bacteria. The absence of EssC in the bacterial membrane could also disturb cell envelope homeostasis, possibly resulting in the mislocalization of some surface proteins that could induce an increased virulence. However, no difference was observed regarding the capacity of mutants for ESX-1 components to invade or multiply inside host cells as compared to WT *Lm*.

L. monocytogenes is sensitive to a broad range of antibiotics. However, resistance to several antibiotics has been reported [40], as well as multidrug-resistant strains [41]. The ESX-1 system could appear as a potential target for innovative anti-*Listeria* drugs that, by inducing ESX-1-dependent secretion, would be capable to impair the infectious capacity of bacteria but not their viability, significantly reducing the risk of resistance development.

Listeria has maintained this locus in its genome, suggesting that it may probably be helpful in certain conditions, such as resisting to stress encountered in specific environments. However, we were unable to find any difference between the WT and *essC* mutant regarding growth in stress conditions such as low pH (pH 5.5) and high salt concentration (4.5% NaCl) (Fig. S1C). Another reason for the conservation of this locus in the *Listeria* genome could be related to a strain issue. Indeed, we tested here the role of the ESX-1 system in only one specific *Lm* strain (*L. monocytogenes* EGDe), that is one of the most commonly used laboratory strains [42, 43]. Even if EsxA was also shown to be dispensable for *in vitro* and *in vivo* growth of a different widely used *Lm* strain [23, 43], this locus could play important roles in the infection capacity of other *Listeria* strains from different serotypes.

In summary, we demonstrated here that the *Lm* genome encodes a functional ESX-1 secretion system required for the secretion of WXG100 proteins, such as EsxA. In addition, despite

poorly expressed and dispensable for cell invasion, we showed that a working ESX-1 system is detrimental for *Lm* infection *in vivo*. Considering its wide distribution among Gram-positive bacteria and the lack of a convergent phenotypic trait for mutants in this pathway, ESX-1 certainly fulfils different functions that remain to be elucidated.

Materials and methods

Bacterial strains and media.

Lm EGDe (ATCC-BAA-679) and *E. coli* strains were routinely cultured aerobically at 37 ºC in brain heart infusion (BHI, Difco) and Lysogeny Broth (LB) media, respectively, with shaking. The synthetic minimal medium (MM) was prepared as previously described [44]. When appropriate, the following antibiotics were included in culture media as selective agents: ampicilin (Amp), 100 μg/ml; chloramphenicol (Cm), 7 μg/ml (*Lm*) or 20 μg/ml (*E. coli*); erythromycin (Ery), 5 μg/ml. For genetic complementation purposes, colistin sulfate (Col) and nalidixic acid (Nax) were used at 10 and 50 μg/ml, respectively.

Construction and complementation of mutant strains.

lmo0056, lmo0061 and *lmo0063* deletions were performed in the EGD-e background through a process of double homologous recombination mediated by the suicide plasmid pMAD as described [45] using the corresponding oligonucleotides (A-D; Table S1). Genetic complementation of the deletion mutant strains was performed using the phage-derived integrative plasmid pPL2 as described [45] using the respective oligonucleotides (Table-S1). For overexpression, target genes were cloned into the pRB474 vector as described [46]. All plasmid constructs and strains were confirmed by PCR and DNA sequencing.

Western blot analysis of EsxA.

Overnight bacterial cultures grown in static conditions (final OD_{660} ~1.0) were centrifuged (10 000 g, 10 min, 4ºC) and the supernatant filtered using Millipore 0.45 µm filters. A volume of 1.6 ml of 50% trichloroacetic acid was added to 6 ml of the filtered supernatant and incubated for 1 h at 4ºC. The sample was centrifuged (30 000 g, 20 min, 4ºC) and the pellet washed with cold acetone, repeating the centrifugation step in same conditions. The pellet was dried, suspended in 30 µl of PBS pH 7.4 and mixed with 15 µl of 4x Laemmli buffer. A volume of 15 µl was loaded in a 12% SDS-polyacrylamide gel. For total bacterial lysates, the bacterial pellet from 10 ml of culture was suspended in 0.8 ml of PBS pH 7.4 containing 100 µg/ml DNase and protease inhibitors. Bacteria were lysed in a FastPrep-24 homogenizer (MP Biomedicals) (30 s, maximum speed) and cell debris removed by centrifugation (3 000 g, 5 min, 4ºC). A volume of 40 µl of 4x Laemmli buffer was added to 100 µl of supernatant of bacterial lysates, and 10 µl loaded into the gels. Western blotting was performed as described [46] using anti-Myc tag mouse antibody (#clone 9B11, Cell Signalling #2276).

Gene expression analyses.

Bacterial RNAs were isolated from 10 ml of cultures at the desired growth phase. For quantification of cytokine expression in mouse livers, organs were homogenized in RNAlater stabilization solution (Qiagen), quick-frozen in dry ice and stored at -80ºC. Total RNAs were extracted by the phenol-chloroform method as previously described [47], and treated with DNase I (Turbo DNA-free, Ambion) as recommended by the manufacturer. Purified RNAs (1 µg) were reverse-transcribed with random hexamers, using iScript cDNA Synthesis kit (Bio-Rad Laboratories). For qualitative analysis, PCR was performed in 20-µl reactions containing 2 µl of cDNA, 10 µl of MangoMix 2× reaction mix (Bioline) and 0.5 µM of forward and reverse primers (Table S1), using the following protocol: 1 cycle at 95 ºC (5 min), 25 cycles at 95 ºC (30 s), 55 ºC (30 s) and 72 ºC (20 s), and 1 cycle at 72 ºC (5 min). Amplification products were

resolved in 1% (w/v) agarose gel and analyzed in a GelDoc XR+ System (Bio-Rad Laboratories). Quantitative real-time PCR (qRT-PCR) was performed in 20-µl reactions containing 2 µl of cDNA, 10 µl of SYBR Green Supermix (Bio-Rad Laboratories) and 0.25 µM of forward and reverse primers (Table S1), using the following cycling protocol: 1 cycle at 95 ºC (3 min) and 40 cycles at 95 ºC (30 s), 55 ºC (30 s) and 72 ºC (30 s). Each target gene was analysed in triplicate and blank (water) and DNA contamination controls (unconverted DNase I-treated RNA) were included for each primer pair. Amplification data were analysed by the comparative threshold (ΔΔCt) method, after normalization of the test and control sample expression values to a housekeeping reference gene (16S rRNA).

Adhesion and invasion assays.

Adhesion and invasion assays were performed as described [45]. Briefly, Caco-2 (ATCC, HTB-37) and Vero (ATCC, CCL-81) cells were seeded (in triplicate) per 24-well plates (~2×10^5/well) in EMEM 20% foetal bovine serum and DMEM 10% foetal bovine serum, respectively (LONZA), and propagated for 48 h. *Listeria* were grown in BHI to OD_{600nm}=0.8, washed and inoculated at 50 bacteria-per-cell for 1h. For adhesion, cells were washed three times washed, lysed in 0.2% Triton X-100 and viable bacteria were enumerated after plating serial dilutions of the lysates in BHI agar media. For invasion assays, cells were infected for 1h and treated with 20 µg/ml gentamicin for 1h30 before lysis in 0.2% Triton X-100.

Intracellular multiplication.

Mouse macrophage-like J774A.1 cells (ATCC TIB-67) were propagated in Dulbecco's modified Eagle's medium (DMEM) containing 10% fetal bovine serum and infection assays were performed as described [37]. Briefly, cells (~2×10^5/well) were infected for 45 min with exponential-phase bacteria at ~10 bacteria/cell and treated afterwards with 20 µg/ml gentamicin for 75 min. At several time-points post-infection, cells were washed with PBS and

lysed in cold 0.2% Triton X-100 for quantification of viable intracellular bacteria in BHI agar. One experiment was performed with triplicates for each strain and time-point.

Animal infections.

Infections were performed in six-to-eight week-old specific-pathogen-free females as described [48]. Briefly, wild-type BALB/c (Charles River Laboratories) or wild-type IFN-γ knock-out C57BL/6J mice were infected intravenously with 10^4 CFUs in PBS, or starved 12h before gavage inoculation with 10^9 CFUs in PBS containing 150 mg/ml $CaCO_3$. The infection was carried out for 72 h, at which point the animals were euthanized by general anesthesia. The spleen and liver were aseptically collected, homogenized in sterile PBS, and serial dilutions of the organ homogenates plated in BHI agar. Mice were maintained at the IBMC animal facilities, in high efficiency particulate air (HEPA) filter-bearing cages under 12-h light cycles, and were given sterile chow and autoclaved water *ad libitum*.

Ethics Statement.

All the animal procedures were in agreement with the guidelines of the European Commission for the handling of laboratory animals (directive 2010/63/EU), with the Portuguese legislation for the use of animals for scientific purposes (Decreto-Lei 113/2013), and were approved by the IBMC Animal Ethics Committee, as well as by the Direcção Geral de Veterinária, the Portuguese authority for animal protection, under license PTDC/SAU-MIC/111581/2009.

Statistical analyses.

Statistical analyses were performed with Prism 6 (GraphPad Software). Unpaired two-tailed Student's *t*-test was used to compare the means of two groups; one-way ANOVA was used with Tukey's post-hoc test for pairwise comparison of means from more than two groups, or with Dunnett's post-hoc test for comparison of means relative to the mean of a control group. Mean differences were considered statistically non-significant (ns) when p value was above 0.05. For statistically significant differences: *, $p \leq 0.05$; **, $p \leq 0.01$; ***, $p \leq 0.001$.

Acknowledgment:

We thank Rui Appelberg for PhD co-supervision of O.R., J.P. and F.C. and MT.A. We thank S. Lamas (Animal Facility), and P. Magalhaes (CCGEN) from IBMC facilities for technical assistance. This work was supported for the D.C. lab by national funds through FCT - Fundação para a Ciência e a Tecnologia/MEC - Ministério da Educação e Ciência and co-funded by FEDER funds within the partnership agreement PT2020 related with the research unit number 4293, and within the research project Infect-ERA/0001/2013 PROANTILIS. O.R., J.P. and F.C. were supported by doctoral fellowships from FCT (SFRH/BD/28185/2006, SFRH/BD/86871/2012 and SFRH/BD/61825/2009), L.M. by the Santander International Mobility Program and SS by FCT Investigator program (COMPETE, POPH, and FCT). This work was supported for the F.G.-dP. lab by grants BIO2014-55238-R (to M.G.P.) and BIO2013-46281-P (to F.G.-dP.) from the Spanish Ministry of Economy and Competitiveness.

References

1. Schneewind O, Missiakas DM. Protein secretion and surface display in Gram-positive bacteria. Philos Trans R Soc Lond B Biol Sci 2012; 367:1123-39.

2. Simeone R, Bottai D, Frigui W, Majlessi L, Brosch R. ESX/type VII secretion systems of mycobacteria: Insights into evolution, pathogenicity and protection. Tuberculosis 2015; 95 Suppl 1:S150-4.

3. Houben EN, Korotkov KV, Bitter W. Take five - Type VII secretion systems of Mycobacteria. Biochim Biophys Acta 2014; 1843:1707-16.

4. Bottai D, Groschel MI, Brosch R. Type VII Secretion Systems in Gram-Positive Bacteria. Curr Top Microbiol Immunol 2016.

5. Stanley SA, Raghavan S, Hwang WW, Cox JS. Acute infection and macrophage subversion by Mycobacterium tuberculosis require a specialized secretion system. Proc Natl Acad Sci U S A 2003; 100:13001-6.

6. Lewis KN, Liao R, Guinn KM, Hickey MJ, Smith S, Behr MA, et al. Deletion of RD1 from Mycobacterium tuberculosis mimics bacille Calmette-Guerin attenuation. J Infect Dis 2003; 187:117-23.

7. Burts ML, Williams WA, DeBord K, Missiakas DM. EsxA and EsxB are secreted by an ESAT-6-like system that is required for the pathogenesis of Staphylococcus aureus infections. Proc Natl Acad Sci U S A 2005; 102:1169-74.

8. Anderson M, Aly KA, Chen YH, Missiakas D. Secretion of atypical protein substrates by the ESAT-6 secretion system of Staphylococcus aureus. Mol Microbiol 2013; 90:734-43.

9. Anderson M, Chen YH, Butler EK, Missiakas DM. EsaD, a secretion factor for the Ess pathway in Staphylococcus aureus. J Bacteriol 2011; 193:1583-9.

10. Chen YH, Anderson M, Hendrickx AP, Missiakas D. Characterization of EssB, a protein required for secretion of ESAT-6 like proteins in Staphylococcus aureus. BMC Microbiol 2012; 12:219.

11. Burts ML, DeDent AC, Missiakas DM. EsaC substrate for the ESAT-6 secretion pathway and its role in persistent infections of Staphylococcus aureus. Mol Microbiol 2008; 69:736-46.

12. Kneuper H, Cao ZP, Twomey KB, Zoltner M, Jager F, Cargill JS, et al. Heterogeneity in ess transcriptional organization and variable contribution of the Ess/Type VII protein secretion system to virulence across closely related Staphylocccus aureus strains. Mol Microbiol 2014; 93:928-43.

13. Korea CG, Balsamo G, Pezzicoli A, Merakou C, Tavarini S, Bagnoli F, et al. Staphylococcal Esx proteins modulate apoptosis and release of intracellular Staphylococcus aureus during infection in epithelial cells. Infect Immun 2014; 82:4144-53.

14. Garufi G, Butler E, Missiakas D. ESAT-6-like protein secretion in Bacillus anthracis. J Bacteriol 2008; 190:7004-11.

15. Akpe San Roman S, Facey PD, Fernandez-Martinez L, Rodriguez C, Vallin C, Del Sol R, et al. A heterodimer of EsxA and EsxB is involved in sporulation and is secreted by a type VII secretion system in Streptomyces coelicolor. Microbiology 2010; 156:1719-29.

16. Baptista C, Barreto HC, Sao-Jose C. High levels of DegU-P activate an Esat-6-like secretion system in Bacillus subtilis. PLoS One 2013; 8:e67840.

17. Huppert LA, Ramsdell TL, Chase MR, Sarracino DA, Fortune SM, Burton BM. The ESX system in Bacillus subtilis mediates protein secretion. PLoS One 2014; 9:e96267.

440 18. European Food Safety Authority ECfDPaC. The European Union summary report on
441 trends and sources of zoonoses, zoonotic agents and food-borne outbreaks in 2013. European
442 Food Safety Authority, European Centre for Disease Prevention and Control EFSA Journal
443 2015; 13:3991.
444 19. Cossart P. Illuminating the landscape of host-pathogen interactions with the bacterium
445 Listeria monocytogenes. Proc Natl Acad Sci U S A 2011; 108:19484-91.
446 20. Camejo A, Carvalho F, Reis O, Leitao E, Sousa S, Cabanes D. The arsenal of virulence
447 factors deployed by Listeria monocytogenes to promote its cell infection cycle. Virulence
448 2011; 2:379-94.
449 21. Carvalho F, Sousa S, Cabanes D. How Listeria monocytogenes organizes its surface for
450 virulence. Frontiers in cellular and infection microbiology 2014; 4:48.
451 22. Desvaux M, Hebraud M. The protein secretion systems in Listeria: inside out bacterial
452 virulence. FEMS Microbiol Rev 2006; 30:774-805.
453 23. Way SS, Wilson CB. The Mycobacterium tuberculosis ESAT-6 homologue in Listeria
454 monocytogenes is dispensable for growth in vitro and in vivo. Infect Immun 2005; 73:6151-3.
455 24. Schulthess B, Bloes DA, Berger-Bachi B. Opposing roles of sigmaB and sigmaB-
456 controlled SpoVG in the global regulation of esxA in Staphylococcus aureus. BMC Microbiol
457 2012; 12:17.
458 25. Zhang Q, Feng Y, Deng L, Feng F, Wang L, Zhou Q, et al. SigB plays a major role in
459 Listeria monocytogenes tolerance to bile stress. Int J Food Microbiol 2011; 145:238-43.
460 26. Stavru F, Archambaud C, Cossart P. Cell biology and immunology of Listeria
461 monocytogenes infections: novel insights. Immunol Rev 2011; 240:160-84.
462 27. Harty JT, Bevan MJ. Specific immunity to Listeria monocytogenes in the absence of IFN
463 gamma. Immunity 1995; 3:109-17.
464 28. Wurtzel O, Sesto N, Mellin JR, Karunker I, Edelheit S, Becavin C, et al. Comparative
465 transcriptomics of pathogenic and non-pathogenic Listeria species. Mol Syst Biol 2012; 8:583.
466 29. Bergholz TM, Bowen B, Wiedmann M, Boor KJ. Listeria monocytogenes shows
467 temperature-dependent and -independent responses to salt stress, including responses that
468 induce cross-protection against other stresses. Appl Environ Microbiol 2012; 78:2602-12.
469 30. Garmyn D, Augagneur Y, Gal L, Vivant AL, Piveteau P. Listeria monocytogenes
470 differential transcriptome analysis reveals temperature-dependent Agr regulation and suggests
471 overlaps with other regulons. PLoS One 2012; 7:e43154.
472 31. Neuhaus K, Satorhelyi P, Schauer K, Scherer S, Fuchs TM. Acid shock of Listeria
473 monocytogenes at low environmental temperatures induces prfA, epithelial cell invasion, and
474 lethality towards Caenorhabditis elegans. BMC Genomics 2013; 14:285.
475 32. Marr AK, Joseph B, Mertins S, Ecke R, Muller-Altrock S, Goebel W. Overexpression of
476 PrfA leads to growth inhibition of Listeria monocytogenes in glucose-containing culture media
477 by interfering with glucose uptake. J Bacteriol 2006; 188:3887-901.
478 33. Joseph B, Mertins S, Stoll R, Schar J, Umesha KR, Luo Q, et al. Glycerol metabolism and
479 PrfA activity in Listeria monocytogenes. J Bacteriol 2008; 190:5412-30.
480 34. Chatterjee SS, Hossain H, Otten S, Kuenne C, Kuchmina K, Machata S, et al. Intracellular
481 gene expression profile of Listeria monocytogenes. Infect Immun 2006; 74:1323-38.
482 35. Schultze T, Hilker R, Mannala GK, Gentil K, Weigel M, Farmani N, et al. A detailed view
483 of the intracellular transcriptome of Listeria monocytogenes in murine macrophages using
484 RNA-seq. Front Microbiol 2015; 6:1199.

485 36. Toledo-Arana A, Dussurget O, Nikitas G, Sesto N, Guet-Revillet H, Balestrino D, et al.
486 The Listeria transcriptional landscape from saprophytism to virulence. Nature 2009; 459:950-
487 6.
488 37. Camejo A, Buchrieser C, Couve E, Carvalho F, Reis O, Ferreira P, et al. In vivo
489 transcriptional profiling of Listeria monocytogenes and mutagenesis identify new virulence
490 factors involved in infection. PLoS Pathog 2009; 5:e1000449.
491 38. Renier S, Micheau P, Talon R, Hebraud M, Desvaux M. Subcellular Localization of
492 Extracytoplasmic Proteins in Monoderm Bacteria: Rational Secretomics-Based Strategy for
493 Genomic and Proteomic Analyses. PLoS One 2012; 7:e42982.
494 39. Aguilo JI, Alonso H, Uranga S, Marinova D, Arbues A, de Martino A, et al. ESX-1-
495 induced apoptosis is involved in cell-to-cell spread of Mycobacterium tuberculosis. Cell
496 Microbiol 2013; 15:1994-2005.
497 40. Walsh D, Sheridan JJ, Duffy G, Blair IS, McDowell DA, Harrington D. Thermal
498 resistance of wild-type and antibiotic-resistant Listeria monocytogenes in meat and potato
499 substrates. J Appl Microbiol 2001; 90:555-60.
500 41. Soni DK, Singh RK, Singh DV, Dubey SK. Characterization of Listeria monocytogenes
501 isolated from Ganges water, human clinical and milk samples at Varanasi, India. Infect Genet
502 Evol 2013; 14:83-91.
503 42. Glaser P, Frangeul L, Buchrieser C, Rusniok C, Amend A, Baquero F, et al. Comparative
504 genomics of Listeria species. Science 2001; 294:849-52.
505 43. Becavin C, Bouchier C, Lechat P, Archambaud C, Creno S, Gouin E, et al. Comparison of
506 widely used Listeria monocytogenes strains EGD, 10403S, and EGD-e highlights genomic
507 variations underlying differences in pathogenicity. MBio 2014; 5:e00969-14.
508 44. Tsai HN, Hodgson DA. Development of a synthetic minimal medium for Listeria
509 monocytogenes. Appl Environ Microbiol 2003; 69:6943-5.
510 45. Reis O, Sousa S, Camejo A, Villiers V, Gouin E, Cossart P, et al. LapB, a novel Listeria
511 monocytogenes LPXTG surface adhesin, required for entry into eukaryotic cells and virulence.
512 J Infect Dis 2010; 202:551-62.
513 46. Lecuit M, Ohayon H, Braun L, Mengaud J, Cossart P. Internalin of *Listeria*
514 *monocytogenes* with an intact leucine-rich repeat region is sufficient to promote internalization.
515 Infect Immun 1997; 65:5309-19.
516 47. Garcia-del Portillo F, Calvo E, D'Orazio V, Pucciarelli MG. Association of ActA to
517 peptidoglycan revealed by cell wall proteomics of intracellular Listeria monocytogenes. J Biol
518 Chem 2011; 286:34675-89.
519 48. Milohanic E, Glaser P, Coppee JY, Frangeul L, Vega Y, Vazquez-Boland JA, et al.
520 Transcriptome analysis of Listeria monocytogenes identifies three groups of genes differently
521 regulated by PrfA. Mol Microbiol 2003; 47:1613-25.
522 49. Cabanes D, Lecuit M, Cossart P. Animal models of Listeria infection. Curr Protoc
523 Microbiol 2008; Chapter 9:Unit9B 1.
524

525

Figure Legends

Figure 1

The ESX-1 locus. (A) Comparison of ESX-1 loci of *M. tuberculosis, S. aureus*, *L. monocytogenes* EGDe, and other *Listeria* species as indicated. Protein homology percentages relative to *L. monocytogenes* EGDe are indicated under each corresponding encoding gene. (B) Schematic representation showing membrane topology or soluble character of proteins encoded by the *L. monocytogenes, S. aureus* and *M. tuberculosis* ESX-1 locus. (A and B) Genes and proteins are coloured following the same code: red corresponds to WXG100 encoding genes or proteins predicted to be secreted to the extracellular medium; blue indicates genes predicted as encoding soluble cytoplasmic proteins; yellow is related to genes or proteins predicted as transmembrane proteins.

Figure 2

Lm ESX-1 system is weakly expressed but functional. (A) Expression of ESX-1 genes in standard growth conditions. The expression of *esxA, esxB, essC* and *essB* was analysed by RT-PCR on total RNAs extracted from logarithmic cultures grown in BHI at 37°C. *inlA, actA* and *iap* were used as control genes. (B) Expression of *esxA* at exponential (Exp) and stationary (Stat) phase of growth measured by RT-PCR (left panel) and qRT-PCR (right panel). Expression value in stationary phase is expressed relative to the value obtained in exponential growth phase. (C) SigB-independent expression of *esxA*. qRT-PCRs performed on total RNAs extracted from WT and Δ*sigB* strains at the exponential (left panel) and stationary (right panel) phase of growth in BHI at 37°C. *bsh was* used as control gene whose expression is SigB-dependent. Gene expression levels in the Δ*sigB* mutant were normalized to those in the WT. (B and C) Values are mean ± SD (n=3). (D) Secretion of EsxA is dependent on EssC. Detection of

551 myc-tagged EsxA protein (EsxA-myc) in supernatants of *Lm* EGDe+*esxA-myc* (WT+ *esxA-*
552 *myc*) at different stage of growth (OD_{600nm} = 0.7, 1.4 and 1.8) (Left panel), and in total bacterial
553 lysates and supernatants from WT, WT+*esxA-myc*, Δ*essC*, Δ*essC*+*esxA-myc* and
554 Δ*essC*+*essC*+*esxA-myc* strains in exponential growth phase (Right panel).
555
556 **Figure 3**
557 The *Lm* ESX-1 secretion system is dispensable for epithelial cell invasion and intracellular
558 multiplication in macrophages. (A) Entry of the WT, Δ*esxA*, Δ*esxB* and Δ*essC* into Caco-2 and
559 Vero cell lines. Values are expressed relative to WT values arbitrarily fixed to 100%. (B)
560 Intracellular replication behaviour of the WT, Δ*esxA*, Δ*esxB* and Δ*essC* strains in J774 cells.
561 Values are mean ± SD (n=3).
562
563 **Figure 4**
564 *Lm* ESX-1 secretion system is detrimental for *in vivo* infection. Bacterial counts for the WT,
565 Δ*esxA*, Δ*esxB* and Δ*essC* strains, in spleens and livers of BALB/c mice (n=5), 72h after (A)
566 intravenous infection with 10^4 bacteria or (B) oral infection with 10^9 bacteria. Data are
567 presented as scatter plots, which each animal represented by a dot and the mean is indicated by
568 a horizontal line. *, $p \leq 0.05$.
569
570 **Figure 5**
571 EsxA secretion impairs *Lm* infection *in vivo* through an IFN-γ-independent mechanism. (A)
572 Bacterial counts for WT, Δ*esxA* and +*esxA* strains, in spleens and livers of BALB/c mice (n=5),
573 72h after intravenous infection with 10^4 bacteria. (B) Bacterial counts for WT and Δ*essC*+*esxA*
574 strains, in spleens and livers of BALB/c mice (n=5), 72h after intravenous infection with 10^4
575 bacteria. (C) Levels of IFN-γ and TNF-α transcripts measured by qRT-PCR in livers of mice

72h after intravenous infection with either WT or +*esxA* bacteria. Expression levels in +*esxA*-infected livers were normalized to those infected with the WT strain. Values are mean ± SD (n=3). (D) Bacterial counts for WT and +*esxA* strains in spleens and livers of WT and IFN-γ knock-out mice (n=5), 72h after intravenous infection with 10^4 bacteria. *, $p \leq 0.05$; **, $p \leq 0.01$.

Figure S1

(A) Genotype confirmation of *esxA, esxB* and *essC* deletion mutant and corresponding complemented strains by PCR. (B) Growth curves of WT, Δ*esxA,* Δ*esxB,* Δ*esxB*+*esxB,* Δ*essC* and Δ*essC*+*essC* strains at 37ºC in BHI broth. (C) Growth curves of WT and Δ*essC* strains at 37ºC in BHI broth with pH adjusted to 5.5 or supplemented with 4.5% NaCl.

Figure S2

Phenotypic analysis of the *Lm* strain overexpressing *esxA* (+*esxA*). (A) The expression level of *esxA* in the +*esxA* strain was measured by qRT-PCR and is shown relative to its level in WT strain. Values are mean ± SD (n=3). (B) Growth curves of the WT and +*esxA* strains at 37ºC in BHI broth and minimal medium. (C) Caco-2 cell adhesion and invasion by the WT and +*esxA* strains. Values are mean ± SD (n=3) and are expressed as percentage relative to WT values arbitrarily fixed to 100%.

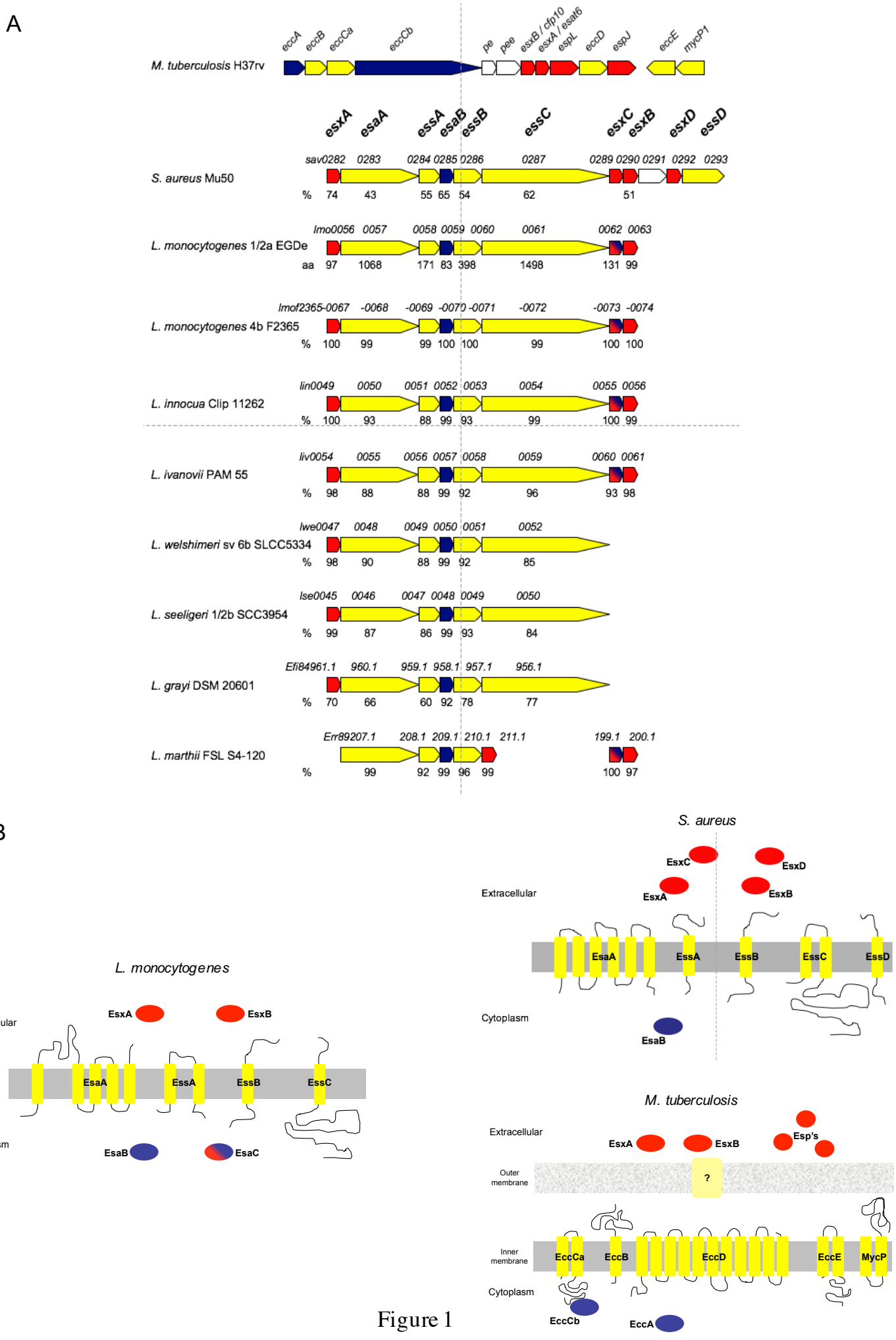
A
eccA eccB eccCa eccCb pe pee esxB / cfp10 esxA / esat6 espL eccD espJ eccE mycP1
M. tuberculosis H37rv
esxA esaA essA esaB essB essC esxC esxB esxD essD
S. aureus Mu50
sav0282 0283 0284 0285 0286 0287 0289 0290 0291 0292 0293
% 74 43 55 65 54 62 51
L. monocytogenes 1/2a EGDe
lmo0056 0057 0058 0059 0060 0061 0062 0063
aa 97 1068 171 83 398 1498 131 99
L. monocytogenes 4b F2365
lmof2365-0067 -0068 -0069 -0070 -0071 -0072 -0073 -0074
% 100 99 99 100 100 99 100 100
L. innocua Clip 11262
lin0049 0050 0051 0052 0053 0054 0055 0056
% 100 93 88 99 93 99 100 99
L. ivanovii PAM 55
liv0054 0055 0056 0057 0058 0059 0060 0061
% 98 88 88 99 92 96 93 98
L. welshimeri sv 6b SLCC5334
lwe0047 0048 0049 0050 0051 0052
% 98 90 88 99 92 85
L. seeligeri 1/2b SCC3954
lse0045 0046 0047 0048 0049 0050
% 99 87 86 99 93 84
L. grayi DSM 20601
Efi84961.1 960.1 959.1 958.1 957.1 956.1
% 70 66 60 92 78 77
L. marthii FSL S4-120
Err89207.1 208.1 209.1 210.1 211.1 199.1 200.1
% 99 92 99 96 99 100 97
B
L. monocytogenes
Extracellular
EsxA EsxB
EsaA EssA EssB EssC
Cytoplasm
EsaB EsaC
S. aureus
Extracellular
EsxC EsxD EsxA EsxB
EsaA EssA EssB EssC EssD
Cytoplasm
EsaB
M. tuberculosis
Extracellular
EsxA EsxB Esp's
Outer membrane
?
Inner membrane
EccCa EccB EccD EccE MycP
Cytoplasm
EccCb EccA

Figure 1

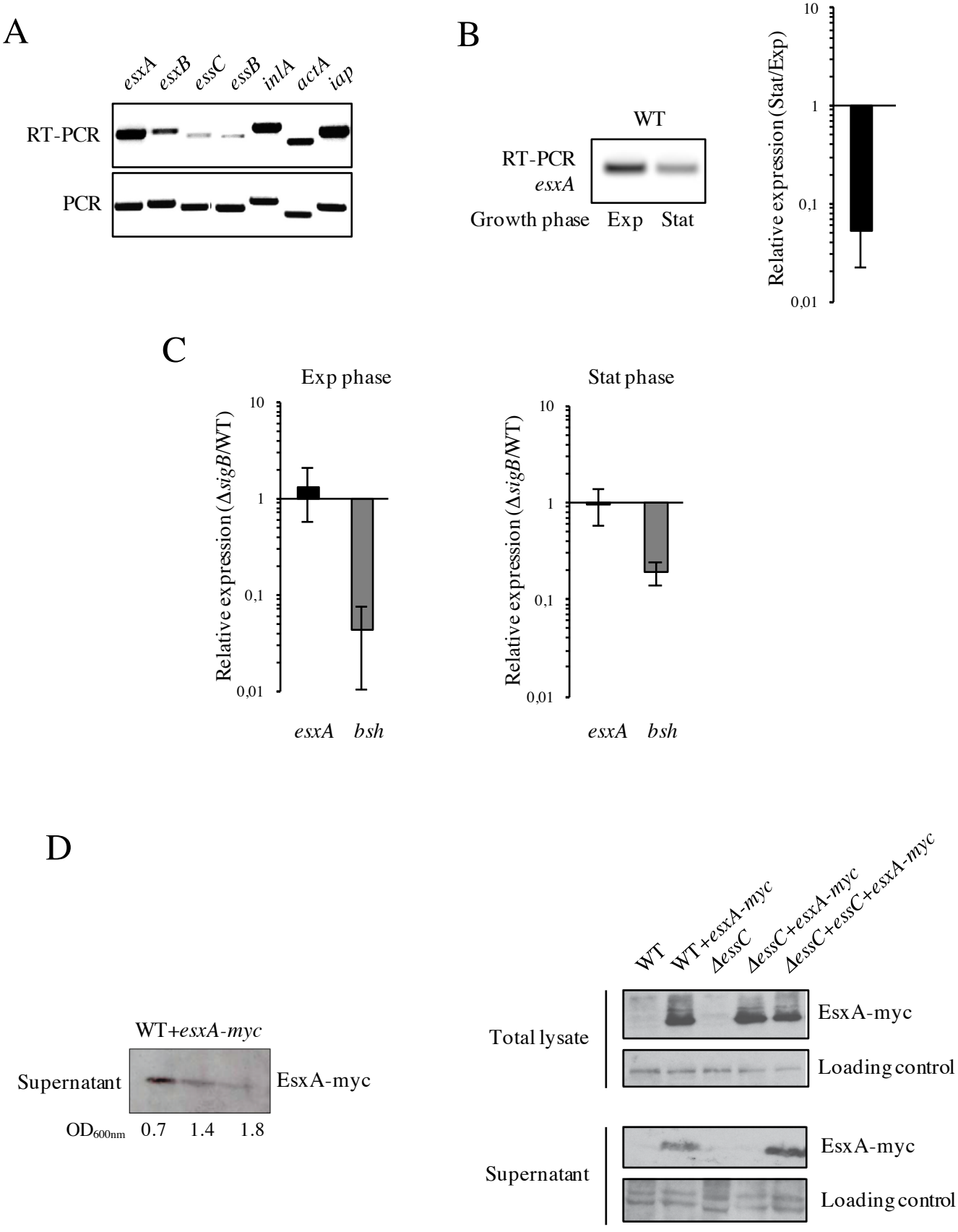
A
esxA
esxB
essC
essB
inlA
actA
iap
RT-PCR
PCR
B
WT
RT-PCR
esxA
Growth phase
Exp
Stat
Relative expression (Stat/Exp)
10
1
0,1
0,01
C
Exp phase
Stat phase
Relative expression (ΔsigB/WT)
esxA
bsh
D
WT+esxA-myc
Supernatant
EsxA-myc
OD600nm
0.7
1.4
1.8
WT
WT+esxA-myc
ΔessC
ΔessC+esxA-myc
ΔessC+essC+esxA-myc
Total lysate
Loading control
Supernatant

Figure 2

A

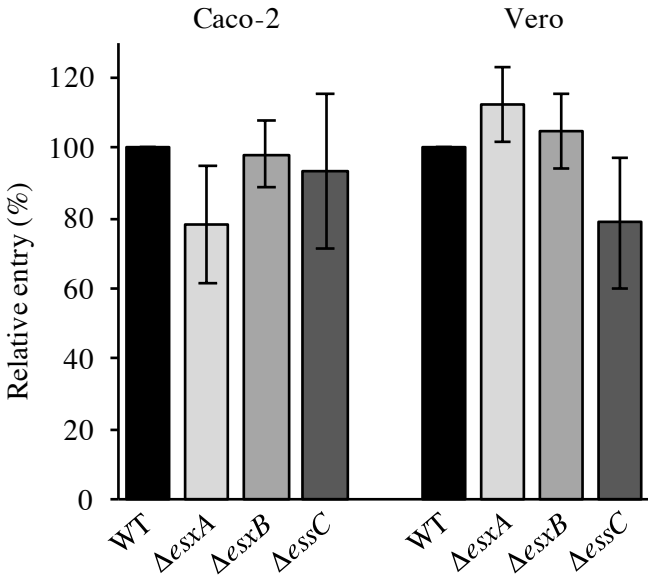
Caco-2
Vero
Relative entry (%)
120
100
80
60
40
20
0
WT
ΔesxA
ΔesxB
ΔessC
WT
ΔesxA
ΔesxB
ΔessC

B

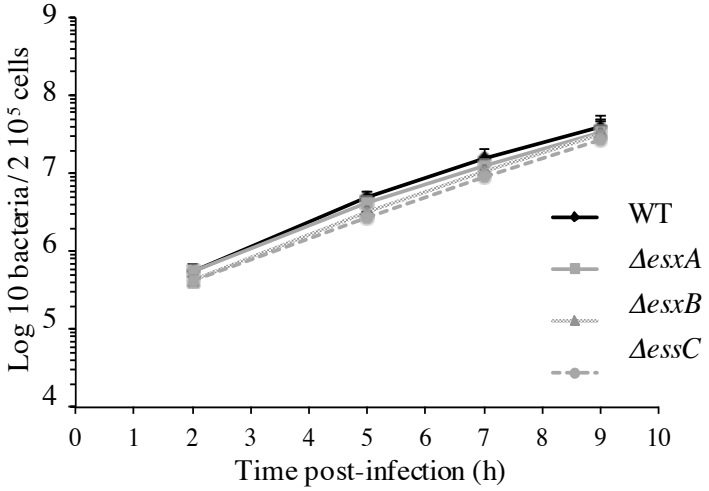
Log 10 bacteria/ 2 10⁵ cells
9
8
7
6
5
4
0
1
2
3
4
5
6
7
8
9
10
Time post-infection (h)
WT
ΔesxA
ΔesxB
ΔessC

Figure 3

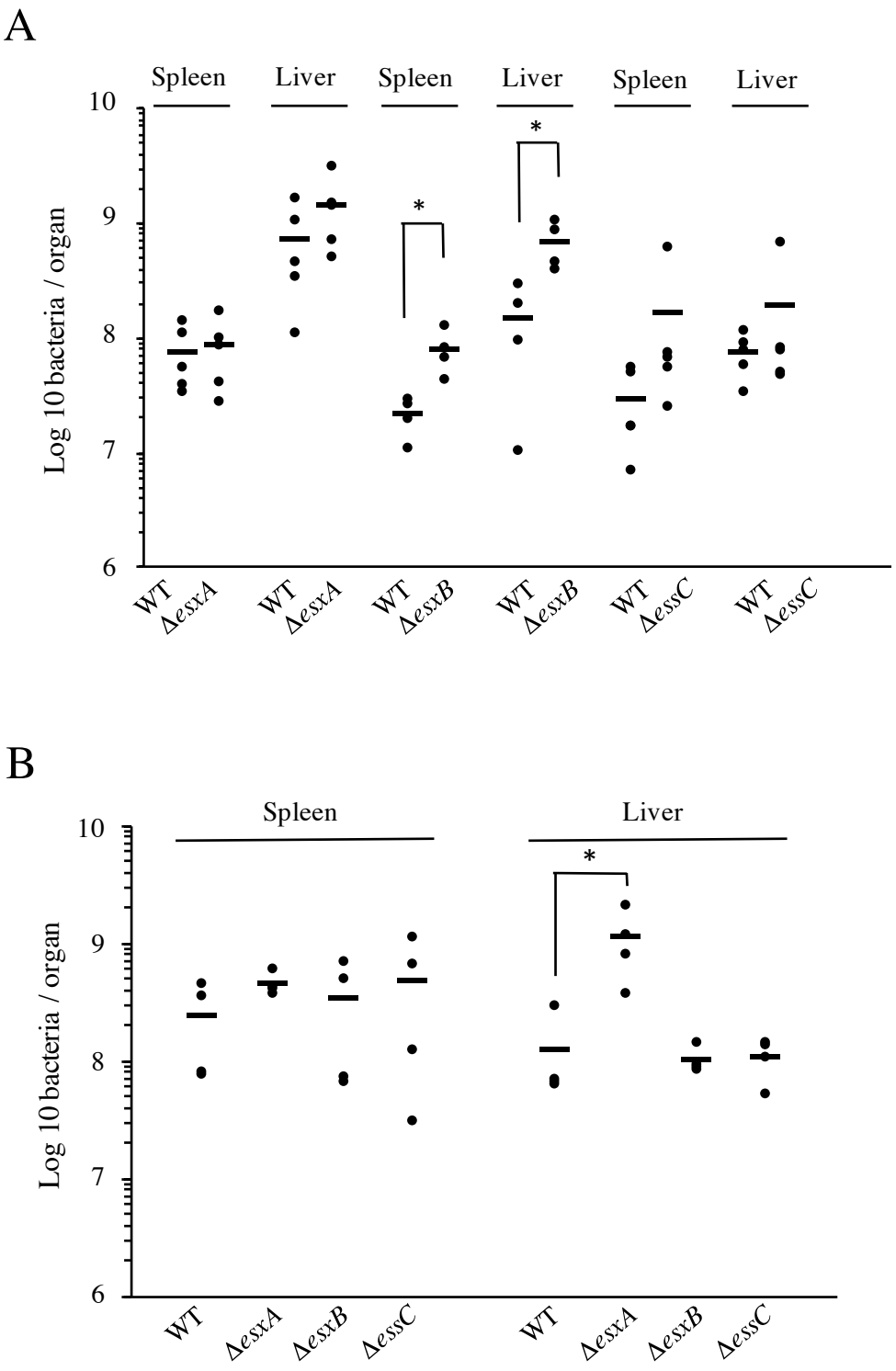
A
Spleen
Liver
Spleen
Liver
Spleen
Liver
10
9
8
7
6
Log 10 bacteria / organ
*
*
WT
ΔesxA
WT
ΔesxA
WT
ΔesxB
WT
ΔesxB
WT
ΔessC
WT
ΔessC
B
Spleen
Liver
10
9
8
7
6
Log 10 bacteria / organ
*
WT
ΔesxA
ΔesxB
ΔessC
WT
ΔesxA
ΔesxB
ΔessC

Figure 4

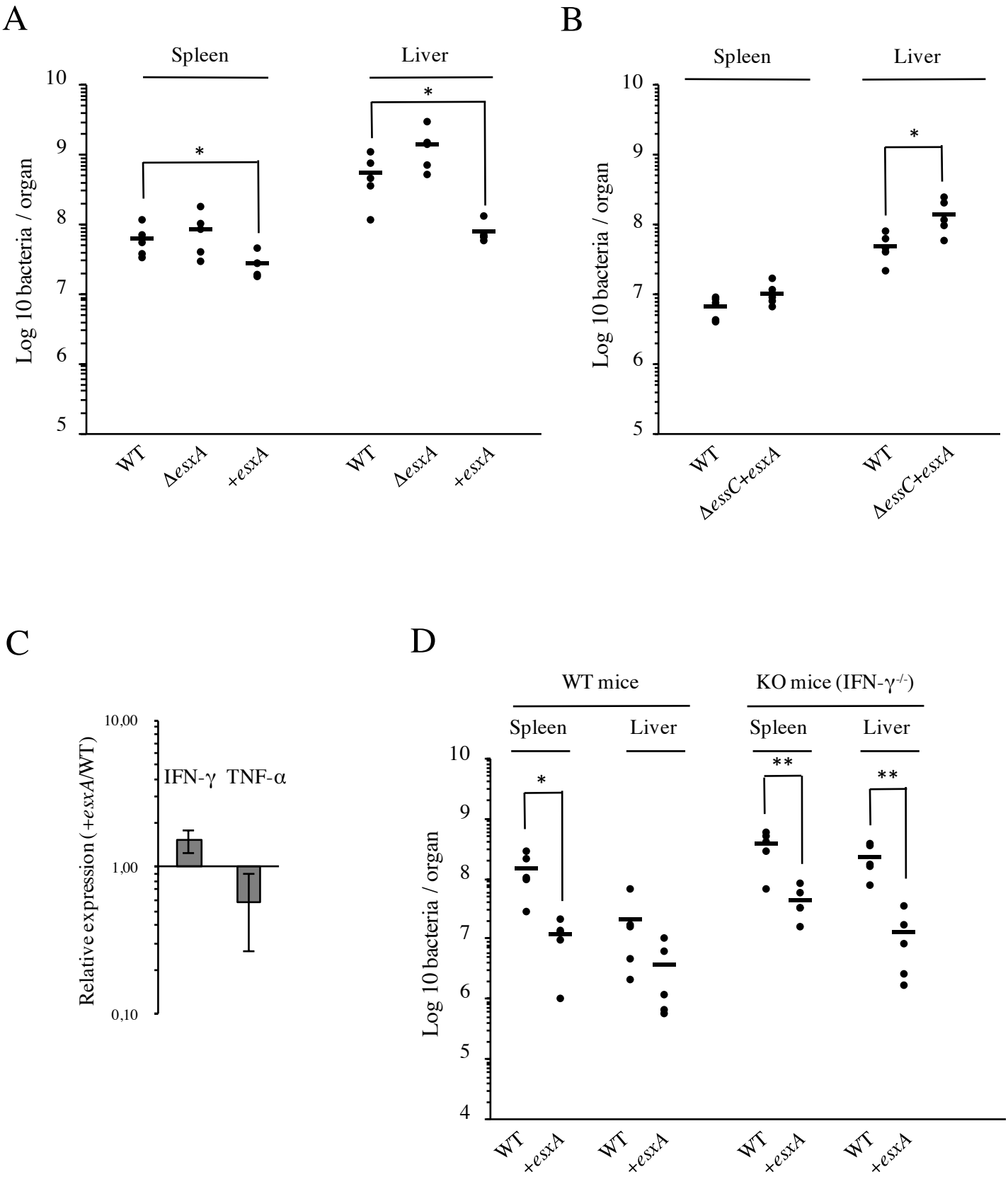
A
Spleen
Liver
Log 10 bacteria / organ
10
9
8
7
6
5
*
*
WT
ΔesxA
+esxA
WT
ΔesxA
+esxA
B
Spleen
Liver
Log 10 bacteria / organ
*
WT
ΔessC+esxA
WT
ΔessC+esxA
C
Relative expression (+esxA/WT)
10,00
1,00
0,10
IFN-γ TNF-α
D
WT mice
KO mice (IFN-γ-/-)
Spleen
Liver
Spleen
Liver
Log 10 bacteria / organ
10
9
8
7
6
5
4
*
**
**
WT
+esxA
WT
+esxA
WT
+esxA
WT
+esxA

Figure 5

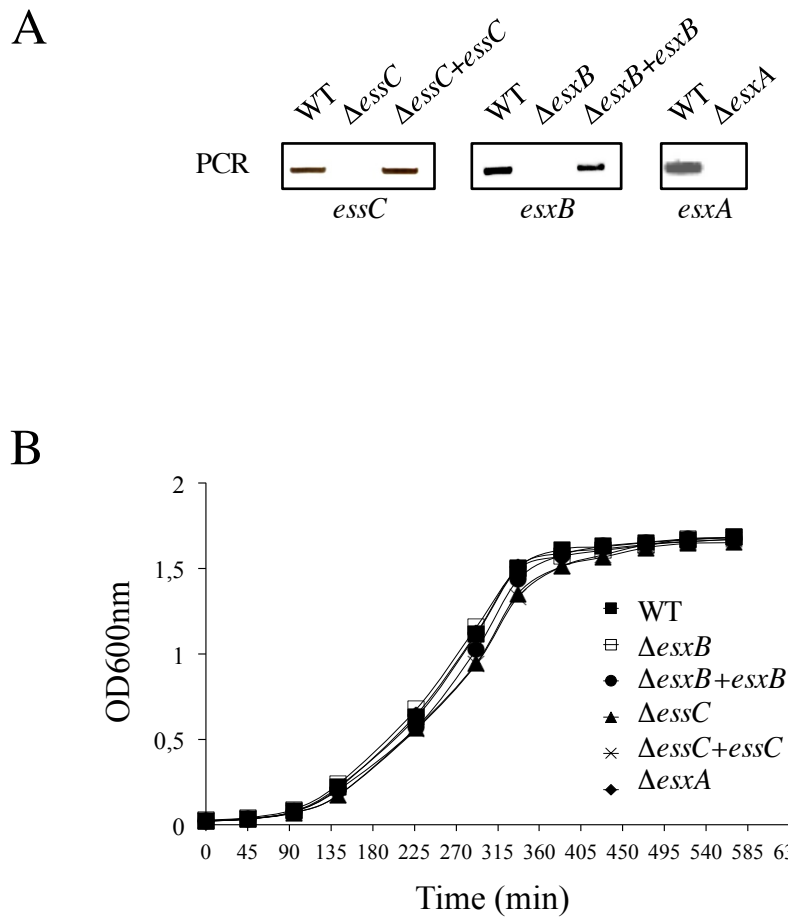
A
WT
ΔessC
ΔessC+essC
WT
ΔesxB
ΔesxB+esxB
WT
ΔesxA
PCR
essC
esxB
esxA
B
OD600nm
Time (min)
WT
ΔesxB
ΔesxB+esxB
ΔessC
ΔessC+essC
ΔesxA
C
pH=5.5
4.5% NaCl
OD600nm
Time (min)
WT
ΔessC

Figure S1

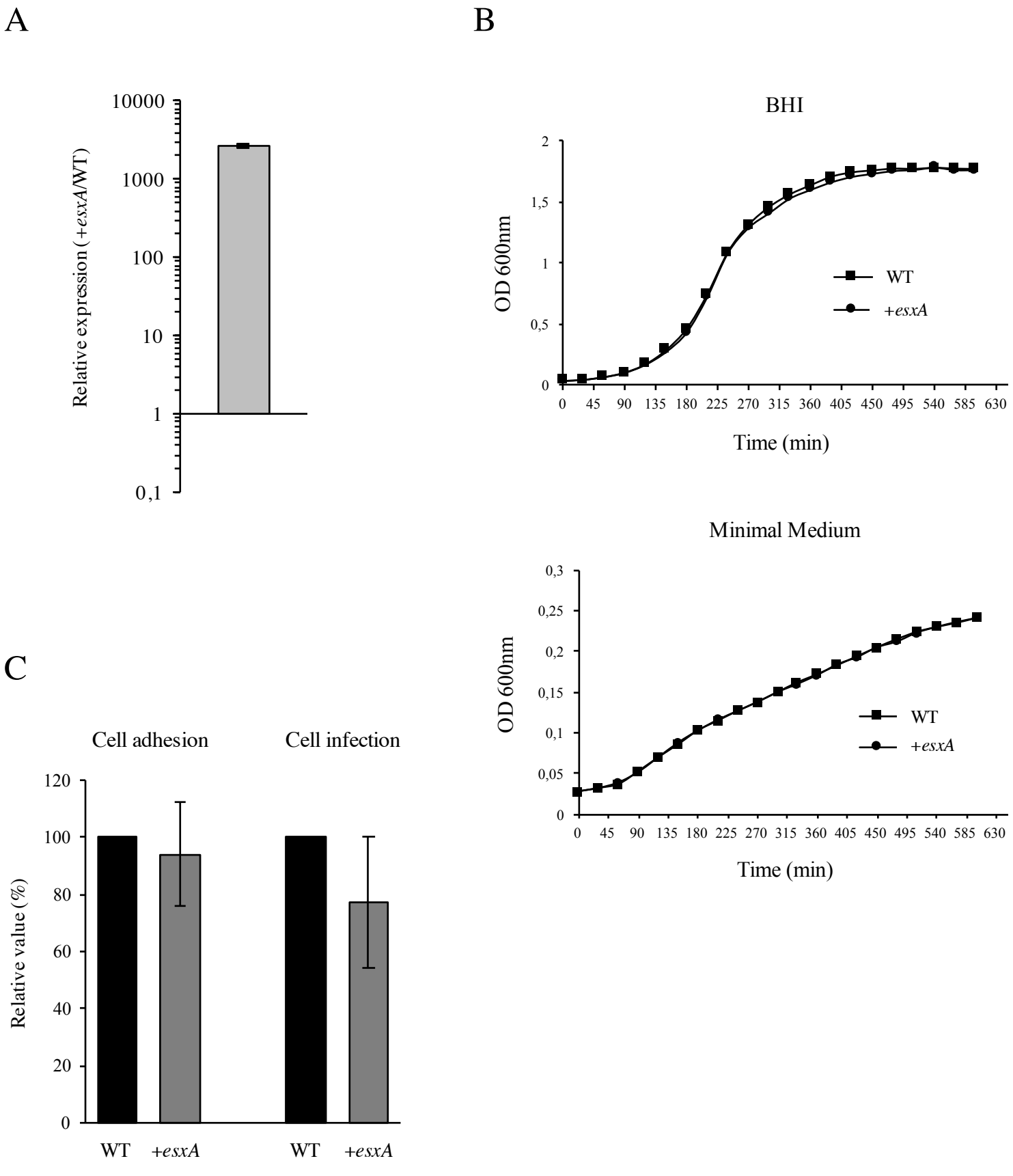
A
B
C
10000
1000
100
10
1
0,1
Relative expression (+esxA/WT)
BHI
OD 600nm
Time (min)
WT
+esxA
Minimal Medium
Cell adhesion
Cell infection
Relative value (%)
WT
+esxA

Figure S2

Table S1 - Oligonucleotides

Name	Sequence (5' > 3')
lmo0063-A	atgtggatcctgaactaattggtcagaatatgg
lmo0063-B	gattacgcgttctttagcctctcctctcgttc
lmo0063-C	ttacgcgtcagtggaaacgatagacgtattttca
lmo0063-D	caagagatcttcatagtcttttcacatccttgg
lmo0056-A	cggatcccgctttagatgatgg
lmo0056-B	gtacgcgtcattcacttcatcacc
lmo0056-C	cgacgcgttaaaatcaacaaaaagtgg
lmo0056-D	cagagatctaagttttctgtgaattctgc
lmo0061-A	caggtcgacacaagttcgaaaaatgggacg
lmo0061-B	agacgcgtggtccattctcccttattttgc
lmo0061-C	cgacgcgttgaaaggagctgttaatgatgg
lmo0061-D	ggaattctcattgggtgtttttttctag
lmo0056-RT-PCR Fw	ggtcaaattcgtatgagtcca
lmo0056-RT-PCR Rv	atcgtgctcttctactgcgtttgc
lmo0058-RT-PCR Fw	gggagttctcgctgcggattcag
lmo0058-RT-PCR Rv	aagtgagtctttaatccggtca
lmo0060-RT-PCR Fw	cttgtacaatggctcgctatcagg
lmo0060-RT-PCR Rv	agcgacgataatgaaaccaaccg
lmo0061-RT-PCR Fw	tgggcatttagctgtgttttctagtc
lmo0061-RT-PCR Rv	attctagtgttaagcgacgaataag
lmo0063-RT-PCR Fw	ggtaatgtgaaaattgatgccgc
lmo0063-RT-PCR Rv	gagtatgaagtattctcaaaatcc